

## **Chapter 5**

**ATP and glutamate released from activated astrocytes via P2X7R induce Tat mediated indirect neuronal death**

## 5.1. Introduction

Purinergic and glutamatergic signaling play key role in synaptic modulation and neuronal excitability in the central nervous system (Haydon, 2001; Fields and Burnstock, 2006). Astrocytes and neurons express the range of purinergic and glutamatergic receptor. Glial cells, especially astrocytes, are considered to be the active player in ATP and glutamate signaling. ATP and glutamate traverse in the astrocytic network following calcium waves and triggers the release of various gliotransmitters including ATP and glutamate themselves (Bernstein et al., 1998; Jeremic et al., 2001). The released ATP and glutamate either act on astrocytes or binds to their particular receptors on neurons that ultimately results in modulating neuronal activity. The glutamate released from astrocytes activates synaptic NMDA receptor or extrasynaptic non-NMDA receptor, whereas ATP acts on P2X or P2Y receptor on neuron whereas after the delayed conversion of ATP to adenosine it binds to P1 receptor causing neuronal suppression. Thus, ATP and glutamate are the major candidates for bidirectional communication within neuron-glia network that is regulated for normal brain functions (Fellin et al., 2006b).

The concentration of glutamate in the neuronal cytosol is in the millimolar range. In the extracellular space, the glutamate concentration is maintained within the physiological range (nanomolar range) by glutamate transporters expressed on astrocyte (Anderson and Swanson, 2000). Glutamate uptake by astrocytes through glutamate transporters (EAAT1 and EAAT2) normally prevents excitotoxic glutamate elevations in brain extracellular space. Decrease in expression of glutamate transporters during injury or disease enhance extracellular glutamate (Benarroch, 2010; Takahashi et al., 2015). Additionally, increased glutamate efflux from astrocytes also adds on to extracellular glutamate which in turn binds to and over stimulates neuronal glutamate receptors (NMDAR/AMPA), enhances intracellular calcium influx and ultimately contributes to neuronal damage (Lau and Tymianski, 2010).

Glutamate excitotoxicity is thought to be one of the several mechanisms by which HIV or the viral proteins like gp120 and Tat exerts neurotoxic effects that culminate in HIV-associated neurocognitive disorders (HAND). Indeed, HIV-1 infected patients show elevated levels of glutamate in CSF that correlate with the severity of dementia and the degree of brain atrophy (Ferrarese et al., 2001). Excess glutamate is released from macrophage/microglial cells upon HIV infection. In infected macrophage, the mitochondrial glutaminase causes excess glutamate release which in turn leads to caspase activation and neuronal cell cycle reactivation, NMDAR overstimulation and subsequent neuronal loss (Zhao et al., 2004; Tian et al., 2008). In astrocytes, the viral protein gp120 and gp41 not only increase the release of glutamate from infected astrocytes but also reduce glutamate uptake. It has been shown that HIV-1 or gp120 down modulates the transcription of EAAT2 transporter gene and thereby, attenuate glutamate uptake by astrocytes (Wang et al., 2003). Since in the brain, astrocytes are intimately connected with neurons, the increased extracellular glutamate pose toxic effect on the nearby neurons by over-activation of glutamate receptor (Vesce et al., 1997; Kort, 1998). Tat protein also induces the release of glutamate from microglial cells which can be controlled by inhibitors of p38 and p42/44 MAPK, NADPH oxidase and the x(c)(-) cystine-glutamate antiporter (Zhao et al., 2004; Gupta et al., 2010). In addition, Tat also leads to depolarization induced increase in glutamate exocytosis from presynaptic nerve terminals which was inhibited upon antagonizing metabotropic glutamate receptor mGlu1 and mGlu5 on neuron (Karlsson et al., 1991; Musante et al., 2010). Tat induces the formation of LRP-PSD95-NMDAR-iNOS complex promoting apoptosis in NMDAR positive and negative neurons and astrocytes (Eugenin et al., 2007). Tat also enhances the glutamate excitotoxicity by direct phosphorylation of NMDA receptors (Haughey et al., 2001).

In clinical practice NMDAR antagonists are being used as adjuvant therapy to treat HAD but the clinical outcomes are not better than HAART as blocking the glutamatergic signaling in the brain has its own side effects, as glutamatergic signaling is important for normal brain function (Lipton, 1994). Another approach is to target enzymes which convert glutamine to glutamate such as glutaminase or to regulate

glutamate transporters; however, trials with such approaches are in early stages and need to be examined further. Another approach can be attenuation of excess glutamate released from astrocytes upon exposure to the virus or viral proteins. Astrocyte-mediated glutamate release occurs in a calcium-dependent manner which involves tightly regulated exocytosis (Jourdain et al., 2007). In addition, several calcium-independent mechanisms also contribute to glutamate release from astrocytes. But the pathways involved in this process are not very clear. Some studies performed on mouse astrocytes suggest that glutamate release can be induced by extracellular ATP. Stimulation of the glial P2X7 receptor causes significant glutamate release from mouse astrocytes and mediates a sustained glutamate efflux. This results in generating tonic current in CA1 neurons which may have some pathophysiological consequences in the brain (Fellin et al., 2006a).

Like glutamate, ATP release from cells can occur via various mechanisms. ATP release can occur through exocytosis/vesicular, channels, protein transporter mediated or by lytic release (Suadicani et al., 2006; Pangrsic et al., 2007; Zhang et al., 2007b; Liu et al., 2008). In astrocytes vesicular and channel-mediated ATP release mechanisms are well studied (Bal-Price et al., 2002; Coco et al., 2003; Pankratov et al., 2006). In context to channel-mediated ATP release, Cx43 and Panx-1 hemichannels are emerging as prominent regulators (Bao et al., 2004; Scemes et al., 2007; Kang et al., 2008). While multiple lines of evidence support the notion that Panx1 are the major mediators of ATP release under physiological and pathological conditions in astrocytes (Pelegrin and Surprenant, 2006; Chekeni et al., 2010; Iwabuchi and Kawahara, 2011; Cheung et al., 2015), various other reports indicates that connexin-43, not pannexin-1 mediates ATP release under certain pathological conditions (Cotrina et al., 1998; Orellana et al., 2011).

P2X7R has been shown to induce ATP efflux from cultured astrocytes which can be normally inhibited in the presence of gap junction blocker. On the contrary, ATP release observed in spinal cord astrocytes and 1321 N1 cells after exposure to low divalent cation solution did not involve connexin-43 hemichannel activity (Suadicani et

al., 2006). In Alzheimer's disease ATP release from astrocytes occurs through connexin-43 hemichannels which in turn lead to neuronal apoptosis through the opening of pannexin-1 hemichannels in neurons (Orellana et al., 2011). Therefore, P2X7R stimulation may release ATP via several membrane proteins including hemichannels (connexin-43 and pannexin-1). However, it has been difficult to clearly discriminate the involvement of the particular hemichannel in ATP release in a myriad of tissues and cells types.

Recent studies on various CNS cell types have highlighted the importance of ATP and purinergic signaling in HIV neuropathogenesis which is discussed in greater detail in chapter 4. During HIV infection, ATP is locally released from infected macrophages or microglia which not only enhances the viral replication by acting upon P2Y and P2X7 receptor (Hazleton et al., 2012) but also causes significant neuronal injury (Tovar et al., 2013; Sorrell and Hauser, 2014). The role of astrocytes in this regard has not been studied in greater detail, hence this study was necessary.

Under normal conditions, BzATP/P2X7R stimulation leads to glutamate and ATP release from astrocytes (Duan et al., 2003; Fellin et al., 2006a; Suadicani et al., 2006). In our study, we have shown upregulated expression of P2X7R upon exposure to Tat. Furthermore, we demonstrated the involvement of P2X7R in Tat-mediated neuroinflammation and indirect neuronal death. The existing literature and leads from our experimental results further prompted us to investigate whether ATP and glutamate release from cultured astrocytes can be enhanced upon exposure to HIV viral protein, Tat. We also investigated if P2X7R is involved in Tat-induced gliotransmitter release. To approach this, we analytically performed several experiments to see whether P2X7R inhibition by P2X7R antagonists decreased the Tat-induced glutamate and ATP release. We further extended our study and investigated whether inhibiting the action of ATP and glutamate on neuronal purinergic receptor and glutamate receptor, respectively, can prevent neuron from Tat-induced indirect toxicity. In addition, we also checked the possibility of involvement of pannexin-1 or connexin-43 hemichannel in ATP release process as it is believed that the hemichannel opening occurs downstream to P2X7R

activation and can be associated with pore formation. Our experimental data demonstrates that Tat exposure leads to P2X7R activation and hemichannel opening which subsequently lead to ATP release from astrocytes. P2X7R also lead to Tat induce glutamate release from astrocytes. The released ATP and glutamate, in turn, lead to indirect neuronal toxicity which can be suppressed by inhibiting neuronal purinergic and NMDA receptors.

## **5.2. Material and Methods**

### **5.2.1. Materials**

ATP assay kit, glutamate assay kit, carbenoxolone, apyrase, oxATP, APV, suramin, A438079, Probenecid, EtBr and antibodies for Cx43 and  $\beta$ -tubulin were purchased from Sigma-Aldrich (Saint Louis, MO, USA). Antibody for Panx-1 was procured from Novus Biologicals (Littleton, CO, USA) and antibody for GFAP was obtained from Chemicon (Billerica, MA, US). Gap26 was purchased from Tocris Biosciences (Bristol, UK). Smart pool ON Target plus Cx43 siRNA and negative control siRNA was purchased from Dharmacon (Lafayette, CO, USA). Sources for all other reagents have been specified in 3.2.1 and 4.2.1.

### **5.2.2. Methods**

#### **5.2.2.1 Cell culture and treatments**

##### **5.2.2.1.1. Primary human astrocytes**

Human astrocytes were differentiated from primary human NPCs as described before (3.2.2.2.). Astrocytes were pretreated for 30 min with specific P2X7R inhibitor A438079, (20  $\mu$ M), non-specific P2R blocker suramin (100  $\mu$ M), hemichannel blocker carbenoxolone (100  $\mu$ M), pannexin-1 hemichannel blocker probenecid (1 mM), connexin43 hemichannel blocker (Gap26, 100 $\mu$ M) or apyrase (10 U/ml) followed by

treatment with Tat for 10 minute for assessment of ATP release. For siRNA experiments, the knockdown was performed for 24 hr as described in section 5.2.2.6. and then Tat was applied for 10 min and ATP assay was performed. All the treatments were carried along with 100  $\mu$ M ARL 67156 (Sigma-Aldrich, Saint Louis, MO, USA) to inhibit the hydrolysis of ATP by ectoATPases. Analysis of EtBr assay was performed after treatment of astrocytes with 100  $\mu$ M BzATP or 100 ng/ml Tat for 15 min and 5 min, respectively. To determine the role of P2X7R in EtBr uptake astrocytes were pretreated with P2X7R antagonists (100  $\mu$ M oxATP and 20  $\mu$ M A438079), nonspecific P2R antagonist suramin (100  $\mu$ M) for 1 hr and with probenecid (1 mM) for 30 minutes. For assessment of glutamate release, cells were pretreated with BBG (1  $\mu$ M), oxATP (100  $\mu$ M) or A438079 (20  $\mu$ M) for 1 hr followed by treatment with Tat for additional 12 hr.

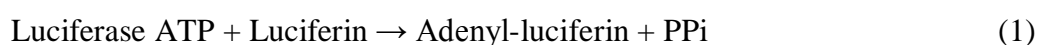
#### **5.2.2.1.2. Primary human neurons**

Human neurons were differentiated from primary hNPCs as described in 4.2.2.1.2. To determine the astrocyte conditioned media induced neuronal apoptosis, astrocytes were treated with 100 ng/ml Tat for 24 hr. 30 min prior to collection of astrocyte supernatant 10 U/ml apyrase (ectoATPase) was added to astrocyte culture media to degrade the extracellular ATP. In parallel cultures of neurons, pretreatment with NMDAR antagonist APV (50  $\mu$ M) or P2R antagonist suramin (100  $\mu$ M) was done for 30 minutes after which half of the neuronal media was replaced with astrocyte conditioned media and kept for 24 hr after which TUNEL assay was performed.

#### **5.2.2.2. ATP release assay**

Astrocytes were cultured in 8 well chamber slide at a density of 20,000 cells/well for 24 hr. Astrocytes were treated with Tat (100 ng/ml) alone or in presence of specific P2X7R inhibitor (A438079, 20  $\mu$ M), nonspecific P2R blocker (suramin, 100  $\mu$ M), hemichannel blocker (CBX, 100  $\mu$ M), pannexin-1 hemichannel blocker (probenecid, 1 mM) or connexin43 hemichannel blocker (Gap26, 100  $\mu$ M). For siRNA experiments, the

knockdown was performed in 24 well plates for 24 hr and then Tat was applied for 10 min. All the treatments were carried along with 100  $\mu$ M ARL 67156 (Sigma-Aldrich, Saint Louis, MO, USA) to inhibit the hydrolysis of ATP by ectoATPases. Supernatants were collected and extracellular ATP in the supernatant was measured using bioluminescent assay kit (Sigma-Aldrich, Saint Louis, MO, USA) which employs the luciferin-luciferase ATP-dependent reaction to evaluate ATP release. ATP is consumed and light is emitted when luciferase catalyzes the oxidation of D-luciferin by the following reaction-



When ATP is the limiting reagent, the light emitted is proportional to the ATP present. In brief, for the assay 100 $\mu$ l assay mix was mixed with 100 $\mu$ l sample (culture supernatant) and kept in the dark. After 3 min, luminescence was measured using single tube Sirius Luminometer (Berthold Detection Systems, Germany). ATP release in the extracellular media under different treatment conditions was represented as fold change compared to control.

### 5.2.2.3. Glutamate release measurements

Astrocytes were plated in 8 well chamber slide (20,000 cells/well/200  $\mu$ l) and experiments were performed 24 hr after seeding. Cells were pre-treated with various P2X7R antagonists (1  $\mu$ M BBG, 100  $\mu$ M oxATP and 20  $\mu$ M A438079) for 1 hr followed by exposure to 100 ng/ml Tat for 12 hr. The cell supernatant was collected and immediately used for glutamate measurement. The levels of extracellular glutamate were determined using glutamine/glutamate determination kit (Sigma-Aldrich, Saint Louis, Missouri, USA) as per manufacturer's protocol. This kit is designed for the spectrophotometric measurement of L-glutamine and/or L-glutamate via enzymatic deamination of L-glutamine and dehydrogenation of L-glutamate with the conversion of NAD<sup>+</sup> to NADH which can be determined spectrophotometrically at 340 nm to provide

an indirect quantification of glutamate concentration. The glutamate released by astrocytes to the extracellular milieu under various treatment conditions was estimated and expressed as a percentage control taking control as 100%.

#### **5.2.2.4. EtBr dye uptake assay**

Astrocytes were exposed to 5  $\mu$ M Ethidium bromide (EtBr) in the presence or absence of 100  $\mu$ M BzATP for 15 min or with 100 ng/ml Tat at 37<sup>0</sup>C for 5 min with Hank's Buffered Salt Solution (137 NaCl mM, 5.4 KCl mM, 0.34 Na<sub>2</sub>HPO<sub>4</sub> mM, 0.44 KH<sub>2</sub>PO<sub>4</sub> mM, pH 7.4) containing 1.2 mM CaCl<sub>2</sub> (HBSS-Ca<sup>+2</sup>). Various P2X7R inhibitors and were applied 1hr prior to BzATP or Tat exposure whereas probenecid was added 30 min before treatment. The EtBr dye uptake was examined by epifluorescence using an inverted Fluid Cell Imaging Station (Life Technologies, Carlsbad, CA, USA). The optical fields having 20-25 astrocytes were selected and 7-8 images from random fields were captured for each treatment. Captured images were analyzed with the Image J program (NIH software) where the mean fluorescence intensity of each cell was analyzed and averaged and expressed as mean  $\pm$  SD.

#### **5.2.2.5. Co-Immunoprecipitation**

Astrocytes were cultured on 25cm<sup>2</sup> flask at the density of  $0.4 \times 10^6$  cells for 24 hr. After 24 hr, cells were washed with PBS buffer and lysed in NP-40 lysis buffer [10 mM Tris-HCl (pH 8.0) 150 mM NaCl, 1 mM EDTA, 1% Triton-X-100, 0.5% nonidet P (NP-40), 0.2% EGTA and 0.2% sodium orthovanadate]. About 100  $\mu$ g of cytoplasmic protein was incubated with the anti-P2X7R antibody at 4<sup>0</sup>C for 12 hr. Immunocomplexes were separated by incubation with Protein- A/G Sepharose and Western blotting was performed as described in 3.2.2.8. The blots were incubated with the anti-panx1 specific antibody (1:2000, Novus Biologicals, Littleton, CO, USA). The immunoblots were then incubated with appropriate horseradish peroxidase (HRP)-conjugated secondary antibody (Vector). The membranes were washed with TBST and signals were visualized using an enhanced chemiluminescence reagent (Millipore, Bedford, MA,

USA). Images were captured using Chemigenius Bio imaging System (Syngene, Cambridge, UK) using Gene snap software. The blot was stripped as described before (4.2.2.7.) and reprobbed with anti-P2X7R antibody. Similar protocol was followed for co-immunoprecipitation of P2X7R and connexin43.

#### **5.2.2.6. Connexin-43 knockdown in human astrocytes by small interfering RNA (siRNA)**

siRNA-mediated knockdown of Cx43 was performed in primary human astrocytes using Lipofectamine RNAiMAX (Life Technologies, Invitrogen, San Diego, CA, USA). Different doses of human-specific Cx43 siRNA (20, 40 and 80 nM) or 80 nM scrambled siRNA (On target plus smart pool siRNA, Dharmacon, Lafayette, CO, USA) were used and transfection was carried out in 25cm<sup>2</sup> culture flasks for 24 hr according to the manufacturer's protocol. The specific silencing of Cx 43 was confirmed by Western blot analysis. 40 nM concentration of Cx43 siRNA showed significant knockdown and was scaled down 4 times for treatments given in 24-well cell culture plates. Further knockdown experiments were carried out in 24 well plates with 10 nM of Cx43 siRNA using equal concentration of scrambled siRNA as control.

#### **5.2.2.7. TUNEL assay**

To assess the toxic effect of ATP and glutamate released from astrocyte on human neurons, human neurons were seeded at a density of 10,000 cells/well in PDL-coated 8-well chamber slides. In parallel cultures, astrocytes were grown in non-PDL-coated 8-well chamber slides at the density of 20,000 cells/well. Astrocytes were treated with 100 ng/ml Tat for 24 hr and, 10 U/ml apyrase was added to astrocyte media 30 min prior to collection of astrocyte supernatant. Simultaneously, cultured neurons were treated with APV (50  $\mu$ M) and suramin (100  $\mu$ M) for 30 minutes and then half of media was replaced with astrocyte conditioned media. Neuronal apoptosis was determined using TUNEL assay as described before (4.2.2.3.). Neurons were labelled with the neuronal marker using anti- $\beta$ III tubulin antibody (Tuj-1) and nuclei were stained with

DAPI. Images were acquired from at least 7 random fields using a Zeiss AxioPlan microscope (Carl Zeiss Company, Heidenheim, Germany) with the charge-coupled device. Apoptotic neurons were expressed as percentage TUNEL positive cells/DAPI.

#### **5.2.2.8. Immunocytochemistry**

Assessment of connexin-43, pannexin-1 and lineage-specific marker GFAP in astrocytes was performed by immunocytochemistry as described in 3.2.2.5. Primary antibody incubation for anti-Cx43 (1:1000) or anti-Panx-1 (1:2000) was done overnight at 4°C. Astrocytes were then incubated with anti-GFAP (1:2000) for 1 hr at RT. Alexa-fluor conjugated secondary antibodies were added in dark for 1 hr at RT. Slides were mounted with Vectasheild mounting medium containing DAPI and images were acquired using Zeiss AxioImager microscope.

#### **5.2.2.9. Western blotting**

After connexin-43 knockdowns, proteins were isolated from astrocytes using NP-40 lysis buffer and Western blotting was performed as described in 3.2.2.8. The membranes were incubated with rabbit anti-Cx43 antibody (1:1000). After overnight incubation at 4°C, membranes were incubated with HRP labelled anti-rabbit secondary antibody. Signal was detected using chemiluminescence reagent (Millipore, Billerica, MA, USA). Images were captured using Chemi Genius Bioimaging System (Syngene, Cambridge, UK) using Gene Snap software. Blots were stripped for 30 min as described in 4.2.2.7. Blots were washed and reprobed with anti- $\beta$ -tubulin (1:3000) as the loading control. Blot images were analyzed using Image J software (NIH, USA) and percentage change was calculated after normalization with respective  $\beta$ -tubulin, taking control as 100%.

#### **5.2.2.10. Statistical analysis**

All the experiments were repeated three to five times and results from each set of experiments were averaged and represented as mean  $\pm$  SD. Statistical significance between groups was calculated using student-‘t’ test. All values of  $p < 0.05$  were taken as significant.

### **5.3. Results**

#### **5.3.1. Treatment of Tat in astrocytes results in release of ATP**

Increased ATP release from HIV-infected macrophages adversely affects the neuronal spine density (Tovar et al., 2013). We, hence, sought to measure the ATP release from the astrocytes following exposure to Tat. The ATP release was measured in the supernatant collected after the treatment of the astrocytes with Tat in the presence of ARL 67156, an ectoATPase inhibitor, which prevents the hydrolysis of the ATP released from the cells. We found a significant increase in ATP release with all the tested doses of Tat (10, 100, 200 and 500 ng/ml) and ATP release was maximum with 100 ng/ml Tat (Fig. 5.1.A). Hence, we chose 100 ng/ml dose of Tat and analyzed the time kinetics for Tat-induced ATP release for which cells were treated in presence and absence of 100 ng/ml Tat for 5, 10, 15 and 30 minutes and the supernatant was collected. We found a significant increase in the extracellular ATP levels after treatment with Tat for 5, 10, and 15 min as compared to controls at similar time points ( $2.49 \pm 0.8$ ,  $3.35 \pm 1.3$  and  $2.95 \pm 0.94$  fold, respectively). In contrast, after 30 min, the Tat-induced ATP change was not significant as compared to the control (Fig. 5.1.B).

#### **5.3.2. Tat-induced ATP release from human astrocytes occurs through activation of purinergic receptors**

ATP release from astrocytes occurs via several mechanisms under different *in vitro* or *in vivo* conditions, including vesicular-mediated release/exocytosis, purinergic receptor-mediated release and lytic release. In an attempt to probe into the mechanism of ATP release following exposure to Tat, we pretreated the astrocytes with A438079 (20 $\mu$ M, a

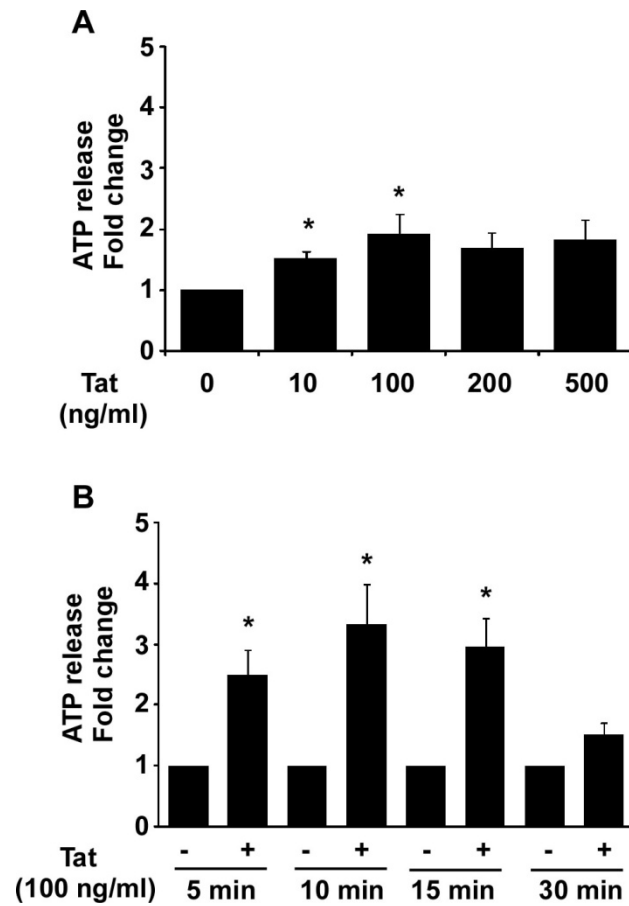


**Figure 5.1. Tat induces the release of ATP from astrocytes.** (A) To check effect of various doses of Tat on ATP release from astrocytes, cells were treated with different doses of Tat (10, 100, 200 and 500 ng/ml) in presence of 100  $\mu$ MARL67156 (inhibitor of ectoATPases) for 15 min. (B) To check the temporal change in ATP release from astrocytes, cells were exposed to 100 ng/ml Tat for indicated time points. The supernatant was collected and ATP release was measured immediately. The control cells were treated with ARL67156 only. The release of ATP from astrocytes was represented as fold change compared to control. The results indicate mean  $\pm$  SD from 4 independent experiments. \* indicates  $p < 0.05$  as compared to respective control.

P2X7R antagonist) for 30 min prior to Tat treatment. We found that P2X7R antagonist significantly reduced the Tat-induced ATP release from  $1.9 \pm 0.16$  to  $0.89 \pm 0.11$ , as shown in Fig. 5.2.A. The release of ATP from astrocytes through P2X7R was further confirmed by knockdown of P2X7R in cultured astrocytes using specific P2X7R siRNA. After 24 hr of knockdown, cells were treated with 100 ng/ml Tat for 10 min and ATP was measured. As expected, P2X7R siRNA also abrogated Tat-induced ATP release from  $1.88 \pm 0.31$  to  $0.88 \pm 0.34$  (Fig. 5.2.B). We then investigated if other purinergic receptors are also involved in the process, for this, we treated astrocytes with 100  $\mu$ M suramin, 30 min prior to Tat treatment. In the presence of suramin Tat-induced ATP release from astrocytes was completely abolished ( $0.008 \pm 0.012$ ). Interestingly, treatment of cells with suramin alone also reduced ATP levels to a larger extent ( $0.012 \pm 0.008$ ). This suggests that the purinergic receptors regulates basal ATP release from astrocytes and are also majorly involved in Tat-induced ATP release. As expected, 10 U/ml of apyrase, an ectonucleotidase, alone or in the presence of Tat completely abolished the amount of ATP ( $0.014 \pm 0.019$  and  $0.006 \pm 0.005$  respectively) in the extracellular media as it hydrolyzes ATP to ADP and AMP which were not detected by the ATP assay kit (Fig 5.2.C).

### **5.3.3. Human fetal brain-derived astrocytes express connexin-43 and pannexin-1 hemichannels**

Connexin-43 and Pannexin-1 are the major hemichannels present on astrocytes (Tovar et al., 2013). We also detected expression of Cx43 and Panx-1 in cultured primary human astrocytes by Western blotting and immunocytochemistry. Western blot analysis revealed that human astrocytes express connexin-43 and pannexin-1 proteins as evident from figure 5.5. Further, the presence of these membrane proteins as gap junction channel or hemichannel cannot be confirmed by Western blotting so we performed double immunostaining to observe their expression with GFAP, an astrocyte marker. We observed that connexin-43 exist in human astrocytes as hemichannels. This was evident from the connexin-43 staining in unopposed astrocyte membranes (Figure 5.3.E.(i)). Connexin-43 also forms gap junction channels upon fusion of two

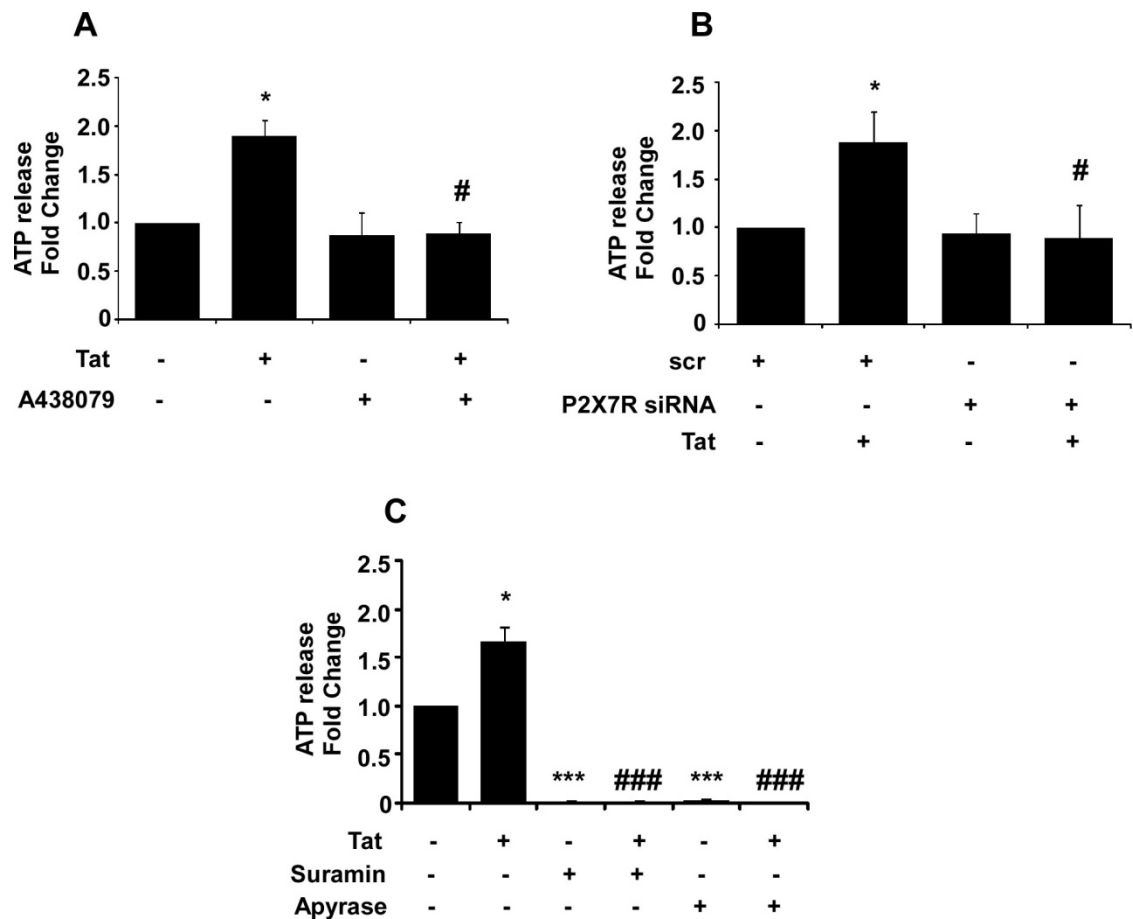


**Figure 5.2. Tat enhances ATP release from human fetal astrocytes via activation of purinergic receptors.** Human astrocytes were exposed to 100 ng/ml Tat for 10 min. To assess the role of purinergic receptors in Tat-induced ATP release, cells were (A) pretreated with 20  $\mu$ M A438079, a potent P2X7R blocker for 30 min prior to Tat treatment. (B) P2X7R knockdown was performed for 24 hr using siRNA against P2X7R (1.6 pmol). For control scrambled siRNA (1.6 pmol) was used. After 24 hr of knockdown, cells were exposed with Tat for 10 min and ATP was measured in the supernatant collected. (C) Cells were pretreated with suramin (100  $\mu$ M), a non-specific P2 receptor antagonist or apyrase (10 U/ml), 30 min prior to exposure to Tat (100 ng/ml). Data represents mean  $\pm$  SD from at least 3 independent experiments in each case. \* and \*\*\* represents  $p < 0.05$  and  $0.001$ , respectively, as compared to respective controls, # and ### represents  $p < 0.05$  and  $0.001$ , respectively, as compared to Tat alone.

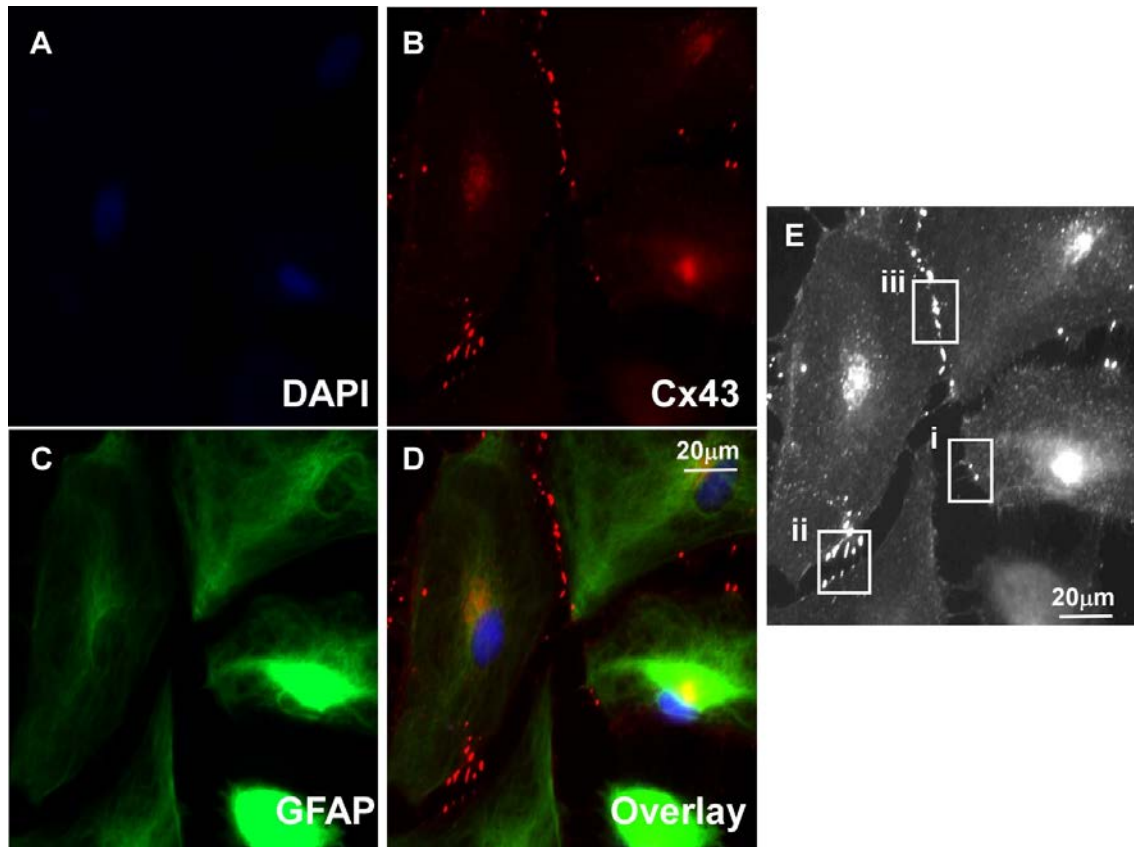


**Figure 5.3. Human fetal astrocytes express connexin 43 gap junction channels and hemichannels.** Astrocyte cultures were triple labelled with (A) nuclear stain DAPI (blue) (B) Connexin 43 (red) and (C) GFAP (green). (D) Shows the co-localization of Cx43 with GFAP (E) The overlay image is represented as the monochromatic image where (i) represents unopposed Cx43 hemichannels on astrocyte membrane (ii) represents unopposed Cx43 hemichannels on two nearby astrocytes. These hemichannels are in close proximity to each other but did not form the gap junction (iii) represents the Cx43 gap junction channels which interconnect two nearby astrocytes and were formed when two hemichannels on the adjacent astrocytes joined together across a cell membrane. Scale bar represents 20µm.

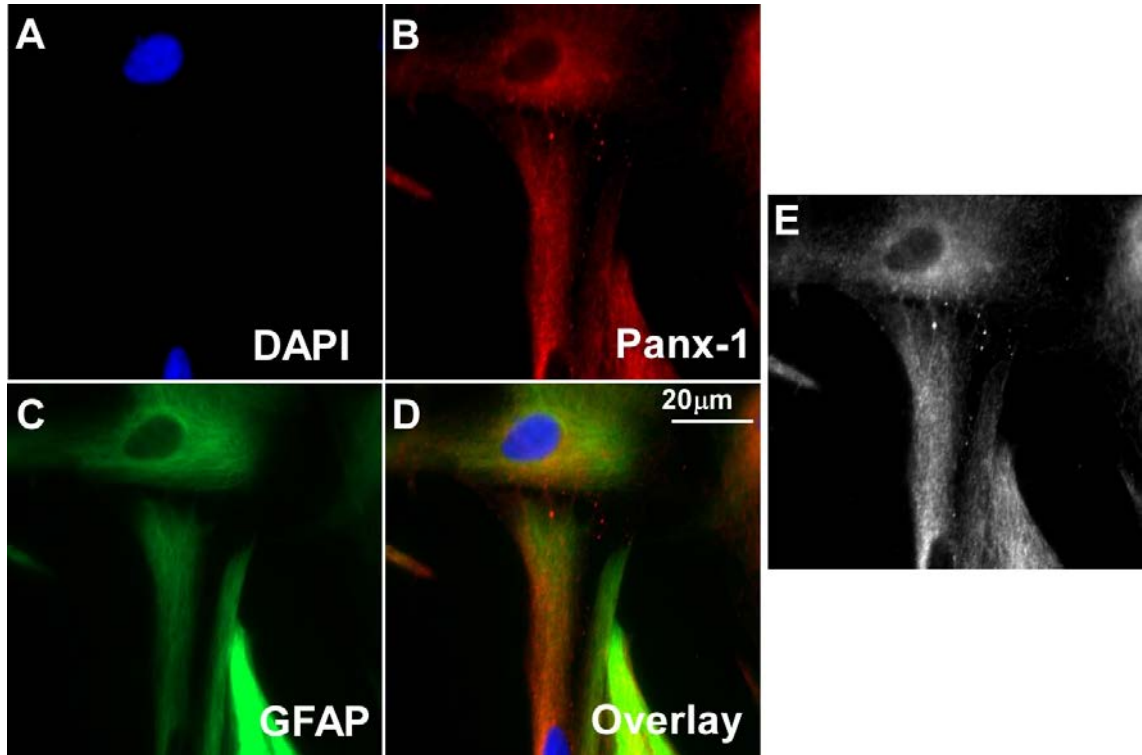


**Figure 5.4. Expression of pannexin-1 hemichannels in human fetal astrocytes.** Astrocyte cultures were triple labelled with (A) nuclear stain DAPI (blue) (B) pannexin-1 hemichannel (red) (C) GFAP (green). (D) shows the co-localization of pannexin-1 with GFAP. (E) The overlay image is represented as the monochromatic image. Scale bar represents 20 $\mu$ m.

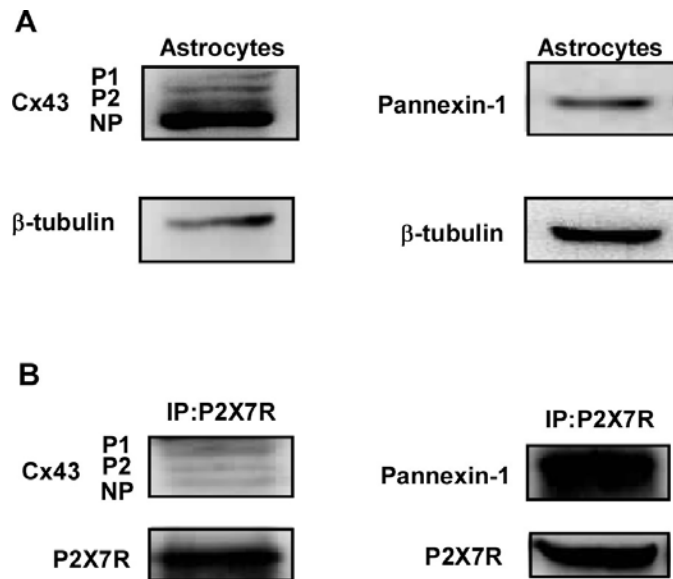


**Figure 5.5. Connexin-43 and Pannexin-1 proteins physically interact with P2X7R in human astrocytes.** (A) Represents expression of Cx43 and Panx-1 on human fetal brain-derived astrocytes at the protein level as determined by Western blot. (B) Co-immunoprecipitation assay was performed for which total protein was isolated from astrocytes. 100  $\mu$ g of protein sample was incubated with anti-P2X7R antibody (IP: P2X7R) overnight at 4°C and Western blot analysis was conducted using anti-Panx1 or anti-Cx43 antibodies. Blots were re-probed with the anti P2X7R antibody. Co-immunoprecipitation assay confirmed P2X7R-Panx1 and P2X7R-Cx43 complex formation in human astrocytes.

hemichannels on adjacent membranes as clearly visible in (Fig. 5.3. E.(ii)). Human astrocytes also expressed pannexin-1 hemichannels. In accordance with the literature, we did not find any gap junction formation with Panx-1 hemichannel (Fig. 5.4.). Experimental evidence suggests that P2X7 activation leads to opening of the hemichannels as a downstream signaling event, hence, we thought that they might be playing some role in P2X7R associated pore formation or ATP release. Hence, we first conducted co-immunoprecipitation (Co-IP) assay to analyze the P2X7R-Panx1 or P2X7R-Cx43 complex formation in astrocytes using the anti-P2X7R antibody as bait to immunoprecipitate Panx-1 and Cx43. As shown in Fig. 5.5.B, Western blot analysis revealed that P2X7R efficiently coimmunoprecipitates Panx-1 thus confirming the presence of P2X7R-Panx-1 and P2X7R-Cx43 complex formation in astrocytes. To the best of our knowledge, this is the first report showing the structural interaction of P2X7R with connexin-43 which may be of some functional relevance and need to be studied in greater details.

#### **5.3.4. P2X7R activation mediated dye uptake/pore formation is inhibited by blocking either the receptor or Panx-1 hemichannel**

We have shown that human astrocytes in culture express the P2X7 and Panx-1 protein. In addition to this, the coimmunoprecipitation assay confirmed the structural association between these two proteins which form P2X7R- Panx1 complex. While evaluating the functional properties of P2X7R in chapter 3, we have also shown that prolonged P2X7R activation leads to pore formation allowing high molecular weight tracer Lucifer yellow to enter the cells. In this chapter, we extended our study to investigate whether P2X7R or Panx-1 is the pore-forming unit in human astrocytes. For our experiments, we used 5  $\mu$ M ethidium bromide (EtBr) which is a high molecular weight fluorescent tracer that enters in live cells only upon membrane permeabilization. It is otherwise used as a marker for apoptotic cells. Stimulation of astrocytes with 100  $\mu$ M BzATP allows significant entry of EtBr into astrocytes indicating membrane permeabilization or pore formation. The BzATP induced pore formation was significantly reduced upon prior treatment of astrocytes with P2X7R antagonists

A438079 (20  $\mu$ M), oxATP (100  $\mu$ M) and suramin (100  $\mu$ M) for 1 hr, followed by treatment with BzATP for 15 min. Probenecid, a specific Panx-1 hemichannel blocker also efficiently reduced BzATP induced pore formation (Fig. 5.6.). This result suggests that pore formation can be reduced either by inhibiting P2X7R or Panx-1 thus both interacting partners are playing a role. In view of the available literature, there might be a possibility that BzATP modulates the conformation of Panx-1 hemichannel structure leading to the opening of hemichannel as a consequence of P2X7R activation.

### **5.3.5. Tat treatment increases membrane permeability of astrocytes by Pannexin-1 hemichannel and P2X7R**

Our study shows that Tat stimulation leads to upregulation of P2X7R in astrocytes and influx of extracellular calcium into the cell cytoplasm. We further checked if brief stimulation with Tat is also able to induce membrane permeabilization in astrocytes. We observed a huge increase in the fluorescence intensity of Lucifer Yellow and EtBr in astrocytes exposed to Tat as compared to nontreated/control cells (Fig. 5.7.). To further elucidate the underlying mechanism for Tat-mediated membrane permeabilization we measured EtBr uptake in confluent astrocytes in the presence of P2X7R and Panx-1 antagonists. After 5 min Tat treatment, the rate of EtBr uptake in astrocytes was about two times higher as compared to control. Probenecid (the blocker of Panx-1 hemichannels) reduced EtBr uptake to the control level thus suggesting that Tat treatment induces Panx-1 hemichannels opening in astrocytes. Thus, pannexin appears to mediate EtBr uptake after 5 min of exposure to Tat. In addition to probenecid, 1 hr pretreatment with P2X7R inhibitors A438079 or oxATP also suppressed the Tat-induced dye uptake upto control level further confirming that effect of Tat is mediated via P2X7R activation in human astrocytes. Furthermore, pretreatment with suramin decreased dye uptake below control levels suggesting that other purinergic receptors also contribute to Tat-induced membrane permeabilization and are also slightly active under basal conditions (Fig. 5.8.).

### **5.3.6. Tat-mediated ATP release involves opening of connexin-43**

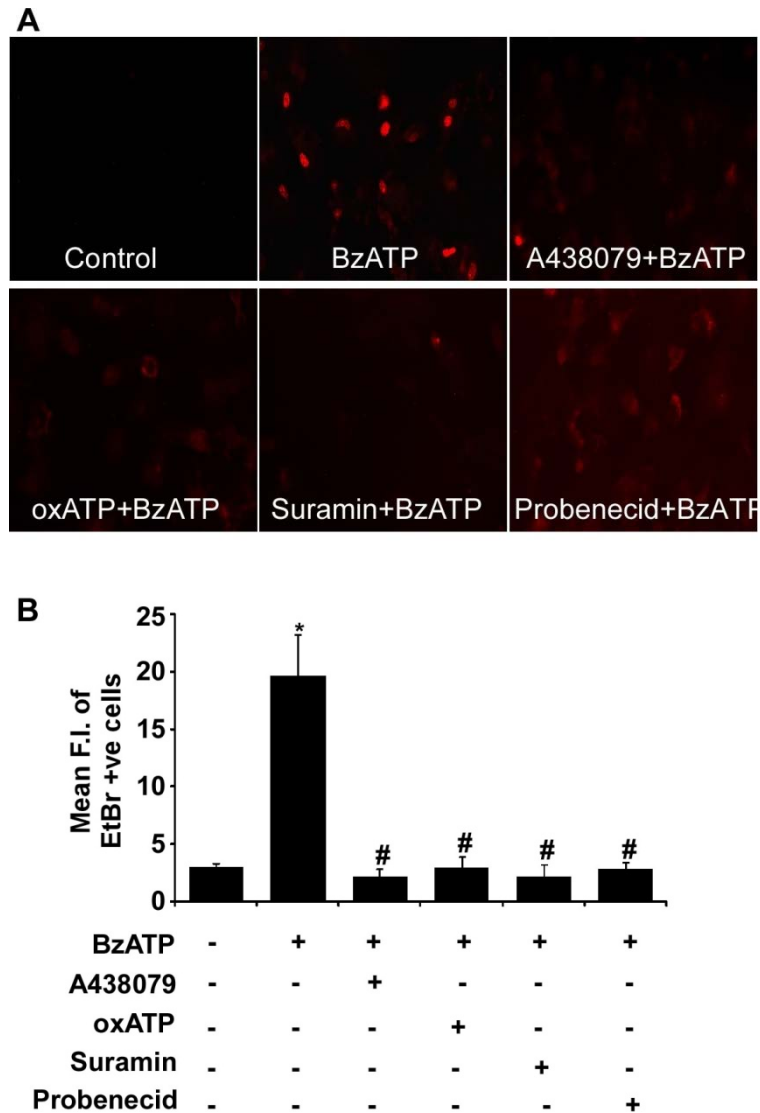


**Figure 5.6. BzATP induces pore formation in astrocytes via activation of P2X7R and pannexin-1 hemichannel opening.** (A) The fluorescent images represent EtBr uptake by human astrocytes in culture. Astrocytes were treated with 100  $\mu$ M BzATP in HBSS buffer in presence of 5  $\mu$ M EtBr. 15 min exposure to BzATP significantly increases EtBr uptake by astrocytes indicating pore formation. Treatment with P2X7R antagonists A438079 (20  $\mu$ M), oxATP (100  $\mu$ M) and P2R antagonist suramin (100  $\mu$ M), 1hr prior to stimulation with 100  $\mu$ M BzATP greatly reduces dye uptake. Pretreatment with probenecid (1 mM), a pannexin-1 hemichannel blocker for 30 min also reduces BzATP induced dye uptake. (B) Represents quantitative analysis of the mean fluorescence intensity of EtBr positive cells. Fields containing 20-25 astrocytes were selected and 7-8 images were captured for each treatment and analyzed using Image J software. Each value corresponds to mean  $\pm$  SD of 150-200 cells from three independent experiments. \* represents  $p < 0.05$  as compared to control and # represents  $p < 0.05$  as compared to BzATP.

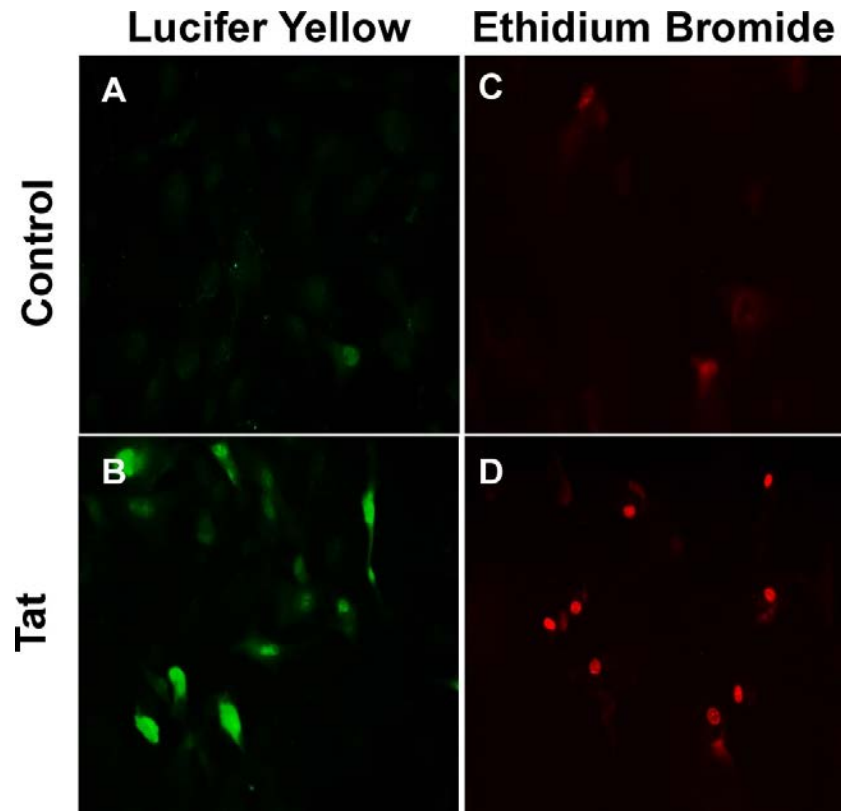


**Figure 5.7. Tat treatment leads to membrane permeabilization in human astrocytes.** Astrocytes were incubated with 1 mg/ml Lucifer yellow or 5  $\mu$ M EtBr in presence or absence of 100 ng/ml Tat. After 5 min, cells were washed with HBSS buffer and immediately observed under a fluorescent microscope. Fluorescent images of astrocytes with Lucifer yellow or EtBr were acquired in control (A & C, respectively.) and Tat treated (B & D, respectively) cells. Tat-induced entry of high molecular weight Lucifer yellow or EtBr into the cells indicates pore formation/increased membrane permeability in astrocytes.

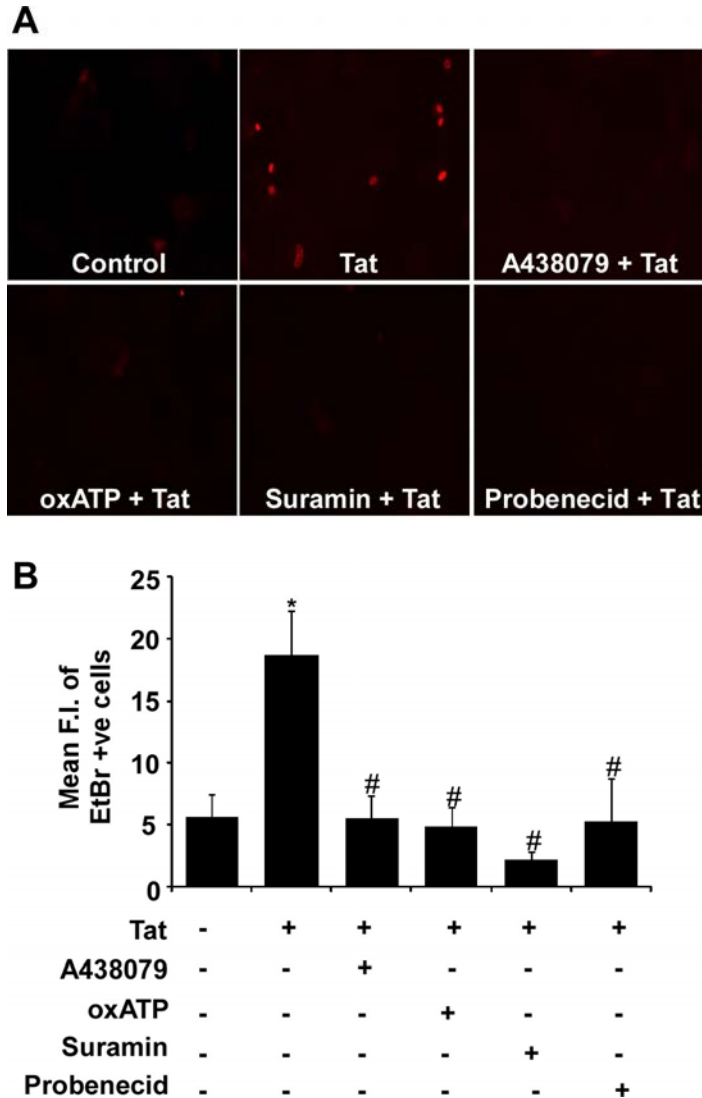


**Figure 5.8. Tat induces increase in EtBr uptake in astrocytes via activation of P2X7R or pannexin-1 hemichannel opening.** (A) Representative fluorescence images of astrocytes showing EtBr uptake by cells under different treatment conditions. Co-application of EtBr (5  $\mu$ M) and Tat (100 ng/ml) for 5 min lead to enhanced dye uptake, representing pore formation in astrocytes. Pre-treatment of cells with P2X7R antagonists A438079 (20  $\mu$ M), oxATP (100  $\mu$ M) and P2R antagonist suramin (100  $\mu$ M), 1hr prior to Tat application significantly reduces dye uptake. Probenecid (1mM), a pannexin-1 hemichannel blocker also decreases EtBr uptake. (B) Represents quantitative analysis of the mean fluorescence intensity of EtBr positive cells. Fields containing 20-25 astrocytes were selected and 7-8 images were captured for each treatment and analyzed using Image J software. Each value corresponds to mean  $\pm$  SD of 150-200 cells from three independent experiments. \* represents  $p < 0.05$  as compared to control and # represents  $p < 0.05$  as compared to Tat.

P2X7R stimulation is associated with ATP release from cells. In our preliminary experiments, we also observed a robust increase in ATP release upon stimulation with BzATP. Several evidence support the notion that P2X7R mediated ATP release occurs via the opening of Pannexin-1 hemichannels as described in 5.1. In our earlier experiments, we showed that Tat induces ATP release from astrocytes via activation of the purinergic receptor. To further investigate the role of hemichannel opening in ATP release process, we pretreated the cells with 100  $\mu$ M carbenoxolone (CBX; pannexin-1 and connexin-43 hemichannel blocker) followed by Tat treatment. As shown in Fig. 5.9.A, CBX pretreatment significantly reduced the Tat-induced ATP release. To specifically demonstrate the Panx-1 hemichannel involvement in the process, we blocked the pannexin-1 hemichannels using probenecid, a specific Panx-1 blocker. Partial inhibition of ATP release through probenecid (although non-significant) suggested that other hemichannels might be involved in the process. Hence, we used Gap 26, a Cx43 mimetic peptide, which blocks the action of Cx 43 and observed that Gap26 reduced the ATP levels to control level (Fig. 5.9. B). To ensure that connexin-43 hemichannels are involved, knockdown of connexin-43 was done by treating the cells with siRNA against human Cx43 (Dharmacon, CO, USA) and checked for the extent of silencing by Western blotting. Western blot analysis revealed significant downregulation of connexin43 after 24 hr siRNA treatment (Fig. 5.10.A & B). Equal concentrations of Cx43 siRNA or scrambled siRNA were used for ATP release assay and Cx43 silencing was performed for 24 hr that was followed by 100 ng/ml Tat treatment for 10 min. Similar to the Cx43 inhibitor, Tat-induced ATP release was significantly reduced in Cx43 siRNA transfected astrocytes and was comparable to control (Fig. 5.10. C). Thus, the results suggest that Tat-mediated ATP release also occurs via Cx43 hemichannels which provide an interesting lead that would require further exploration.

### **5.3.7. Exposure to Tat causes glutamate release from astrocytes via activation of P2X7R**

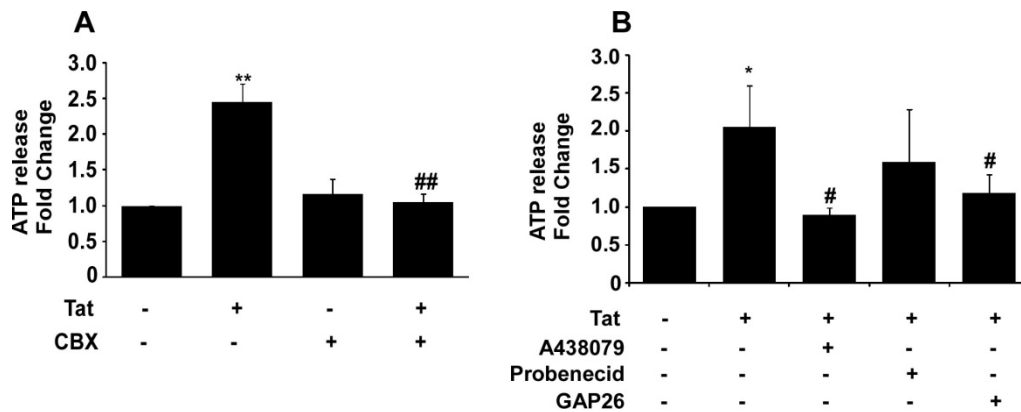


**Figure 5.9. Tat-induced ATP release involves P2X7R activation and Cx43 hemichannel opening.** (A) Treatment of astrocytes with 100 ng/ml Tat showed significant ATP release. Pretreatment of cells with carbenoxolone (CBX, 100  $\mu$ M), a gap junction and hemichannel blocker for 30 min, prior to Tat treatment significantly reduced Tat-induced ATP release. (B) To further investigate the relative contribution of Panx-1 hemichannel or Cx43 hemichannel in Tat-induced ATP release, astrocytes were treated with probenecid (1 mM), a specific hemichannel blocker or Gap26, a connexin 43 mimetic peptide 30 min prior to Tat exposure. The bar the graphs indicate the fold change in ATP release as compared to control. The data represent mean  $\pm$  SD from 4 independent experiments. \*and \*\* indicates  $p < 0.05$  and  $0.005$  as compared to control. # and ## indicates  $p < 0.05$  and  $0.005$  as compared to Tat.

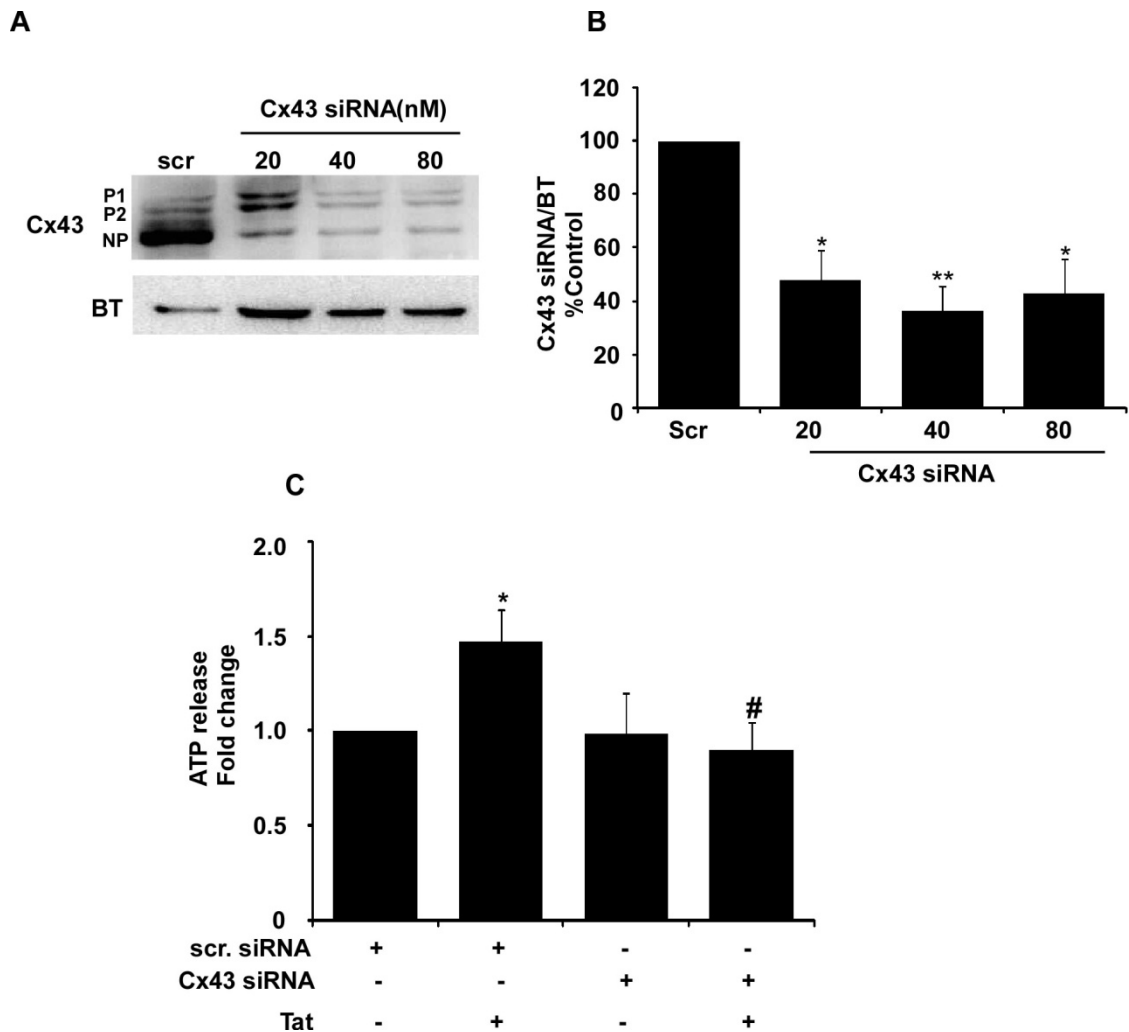


**Figure 5.10. Connexin 43 knockdown in astrocytes decreases Tat-induced ATP release:** Human astrocytes were treated with different doses of Cx43 specific siRNA (20, 40 and 80 nM) using scrambled siRNA (80 nM) as the control. The knockdown was studied by Western blotting. (A) Representative blots showing maximum decrease in connexin 43 expressions with 40 nM concentration of Cx43 siRNA as compared to scrambled control.  $\beta$ -tubulin was used as loading control. For astrocyte treatments in 24 well culture plates the dose of siRNA was scaled down four times (10 nM) and used. (B) Represents the densitometric analysis of blot shown in (A). (C) In 24 well culture plates, astrocytes were pretreated with 10nM scrambled or Cx43 siRNA. After 24 hr cells were exposed with 100 ng/mlTat for 10 min and ATP assay was performed. For comparison, the ATP release in scrambled siRNA treated cells are taken as controls and ATP release is expressed as fold change compared to control. Connexin knockdown in astrocytes significantly attenuated Tat-induced ATP release. Data are expressed as mean  $\pm$  SD of four independent experiments. \* and \*\* indicates  $p < 0.05$  and  $0.005$  respectively; as compared with the controls. # indicates  $p < 0.05$  as compared with Tat treated cells.

Extracellular Tat has been shown to mediate glutamate release from astrocytes and is, in fact a major pathway for astrocytes induced neurotoxicity by overstimulation of neuronal NMDA receptors (Ton and Xiong, 2013). P2X7R activation has also been shown to induce glutamate release from astrocytes (Fellin et al., 2006a). Hence, we sought to identify if Tat-mediated glutamate release is regulated by activation of P2X7R in human astrocytes. For this, astrocytes were pretreated with 20  $\mu$ M A438079, 1  $\mu$ M BBG or 100  $\mu$ M oxATP for 1 hr and then 100ng/ml of Tat was added to the cells for additional 12 hr. After 12 hr, the cell supernatant was collected and glutamate was measured immediately using glutamate-glutamine assay kit. Treatment with Tat significantly increased glutamate releases ( $131 \pm 7.7\%$ ) from astrocytes as compared to nontreated cells/control. Prior treatment with various PX7R antagonists significantly reduced Tat-induced glutamate level near control (Fig. 5.11.) suggesting the involvement of P2X7R in Tat-induced glutamate release.

#### **5.3.8. Death of neurons is mediated by activation of purinergic (P2) and glutamatergic (NMDA) receptors**

Excess glutamate is known to cause neuronal excitotoxicity in HIV neuropathogenesis. ATP released from HIV-infected macrophages has also been shown to affect neuronal health (Tovar et al., 2013). In our study, we found a significant increase in ATP and glutamate release from astrocytes upon exposure to Tat. Confirming the role of P2X7R activation in both the mechanisms, we extended our study to check the possibility if ATP and glutamate released from astrocytes contribute to Tat-treated astrocyte conditioned media (ACM) induced neuronal apoptosis. In accordance with our previous results, exposure of neuronal culture to astrocyte conditioned media (ACM) collected after treatment with Tat increased neuronal death ( $21.94 \pm 5.07$ ) as compared to ACM from non-treated cells ( $2.09 \pm 0.57$ ), as evaluated by TUNEL assay. The increase in Tat-ACM induced neuronal death was reduced upon treatment of astrocytes with 10 U/ml apyrase (an ectoATPase), 30 minutes prior to treatment of neurons with ACM (from  $21.94 \pm 5.07$  to  $4.19 \pm 2.7$ ). Pretreatment of neurons with broad spectrum P2R blocker suramin ( $3.47 \pm 0.43$ ) or NMDA receptor blocker APV ( $3.6 \pm 0.66$ ) reduced

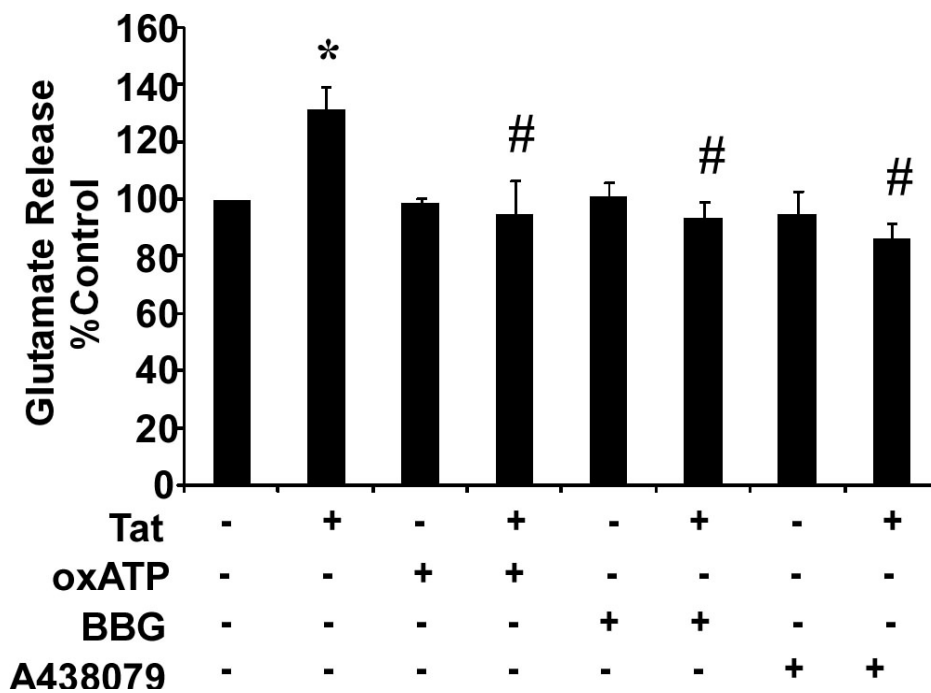


**Figure 5.11. HIV-Tat induces the release of glutamate from astrocytes via activation of P2X7R:** Human fetal astrocytes were treated with 100 ng/ml Tat for 12 hr. After 12 hr supernatant was collected and glutamate release was measured using glutamate –glutamine assay kit. The role of P2X7R in Tat-mediated glutamate release was analyzed by pretreatment of astrocytes with oxATP (100  $\mu$ M), BBG (1  $\mu$ M) or A438079 (20  $\mu$ M), 1hr prior to addition of Tat. The data shows percentage neuronal death taking control as 100%. Data represents mean  $\pm$  SD from 7 independent experiments. \* indicates  $p < 0.05$  as compared to control and # indicates  $p < 0.05$  as compared to Tat.

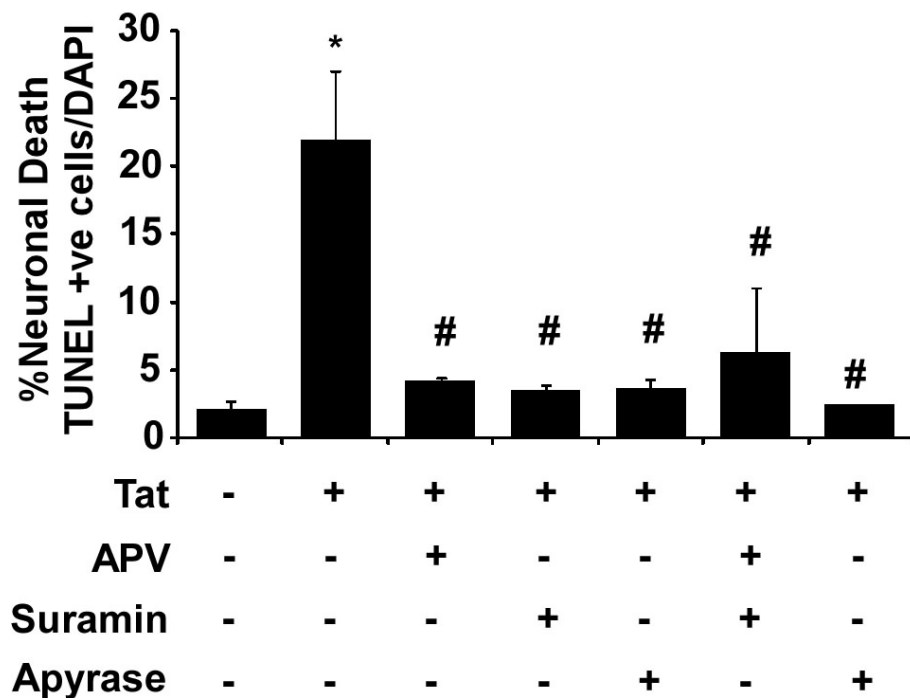


**Figure 5.12. Astrocyte-conditioned media induced neuronal toxicity is mediated via activation of neuronal purinergic and glutamatergic receptor:** Astrocytes were treated with 100 ng/ml Tat for 24 hr Apyrase (10 U/ml), an ectoATPase, which hydrolyze extracellular ATP to ADP and AMP was added to astrocyte culture for the last 30 min, before collecting the supernatant. In pure neuronal culture, half of the neuronal media was replaced with astrocyte conditioned media. Neurons were treated with suramin (100  $\mu$ M) or APV(50  $\mu$ M) for 30 min followed by exposure to astrocyte conditioned media for additional 24 hr. TUNEL assay was used to assess neuronal apoptosis following exposure of neurons to astrocyte conditioned media (ACM) for 24 hr. The data represents percentage neuronal death as determined by counting the number of TUNEL positive and DAPI positive cells and taking the ratio of TUNEL +ve cells/DAPI for each treatment control \* indicates  $p < 0.05$  as compared to control and # indicates  $p < 0.05$  as compared to Tat.

neuronal death to control levels. We did not observe further significant decrease in neuronal apoptosis upon co-application of APV with suramin or apyrase as compared to their treatment alone (Fig. 5.12.).

#### **5.4. Discussion**

Astrocyte activation or dysfunction and neuronal death are the major pathological hallmarks of HIV neuropathogenesis in the central nervous system (CNS). In this study, we demonstrated that Tat treatment to astrocyte leads to significant increase in ATP and glutamate release from astrocytes (Figure 5.1. & 5.11.). Reduction in ATP release upon prior treatment with P2X7R antagonist suggests the involvement of astrocytic P2X7R in the process (Fig. 5.2.A). Silencing the receptor using siRNA against P2X7R further confirmed our experimental results (Fig. 5.2.B). Interestingly, treatment of astrocytes with suramin, non-specific P2 receptor antagonist completely abolished ATP levels in the extracellular media. This suggests that purinergic receptors other than P2X7R are also involved in the basal release of ATP from astrocytes and are the major contributors to the process. Even, Tat treatment was not able to induce ATP release in suramin-treated cells suggesting that Tat also requires activation of other purinergic receptors for ATP release from astrocytes (Figure 5.2.C).

Repeated or prolonged stimulation of cells with BzATP is associated with the formation of a non-selective pore allowing the entry of solutes upto 900Da in size, which eventually leads to membrane blebbing, release of cytokines and cell death (Verhoef et al., 2003; Roger et al., 2008). Studies by Sayar *et al* on P2X7R transfected HEK 293 and RAW 264.7 cells have shown that P2X7 receptors activate at least two permeation pathways, one for cationic (YO-PRO-1 and TO-TO-1) and one for anionic dyes (Lucifer yellow and calcein) with different activation properties (Schachter et al., 2008; Cankurtaran-Sayar et al., 2009). Earlier it was believed that the formation of large pore was due to the dilation of the P2X7R cation channel itself, however, several studies conducted on P2X7R in different cell type suggests that an additional component is required along with the P2X7 receptor for the opening of non-selective

pore (Shoji et al., 2014) as shown in the schematic representation in figure 1.6. Recently, Pelegrin & Surprenant have speculated that the pore formation activity is mediated by Pannexin-1 hemichannels physically attached with P2X7R. This study was also supported by Locovei *et al.* and Iglesias *et al* with strong evidences for the role of Pannexin-1 as a part of pore-forming unit of P2X7 receptor (Pelegrin and Surprenant, 2006; Locovei et al., 2007) proposing the Src tyrosine kinase as a principal mediator of this activation (Iglesias et al., 2008). Interestingly, the study by Bhaskaracharya *et al* has shown that P2X7R mediated pore formation is independent of pannexin-1 hemichannel activity (Bhaskaracharya et al., 2014). Earlier report by Hanley *et al* also observed the same results when increase in intracellular calcium due to transient stimulation of P2X7R lead to cell death in mouse macrophage, however, neither the cell death nor the pore formation was found to be dependent on pannexin-1 hemichannel as pannexin-1 deficiency did not affect any of the mechanism (Hanley et al., 2012). Thus, the physiological role of pore formation because of P2X7R activation is still not clear, however, it is believed that pore formation is downstream to P2X7R activation. Further studies have warranted the need for understanding the functional importance of the P2X7-pannexin-1 interaction under different conditions.

In addition to pore formation, the role of hemichannel activity has also been suggested in ATP release from various cells types. In this regard, connexin-43 hemichannels and Pannexin-1 hemichannels are the most commonly studied hemichannels (Wei et al., 2014; Dahl, 2015). Therefore, we first checked the expression of these two proteins in human astrocyte cultures. From Western blot and immunocytochemistry, we found constitutive expression of Cx43 and Panx-1 in astrocytes. Moreover, immunocytochemical observation from GFAP and Cx43 or Panx-1 colocalization suggested that Cx43 in astrocytes either exists as hemichannel, a single membrane channel or gap junction channel which are formed upon docking of two hemichannels on opposing membrane when the cells come in close contact with each other (Fig. 5.3.). Panx-1 was found to be expressed only as hemichannel and do not form gap junction (Figure 5.4.). We next checked whether the P2X7R forms complex with Panx-1 or Cx43 in cultured astrocytes. The co-immunoprecipitation results

revealed the presence of P2X7R- Panx-1 and P2X7R- Cx43 complex formation (Fig. 5.5.). However, the structural association of P2X7R-Panx-1 was found to be more as compared to the P2X7R-Cx43 association. The P2X7R- Cx43 complex formation has not been reported earlier and provides an interesting lead. Their interaction in astrocytes might be playing an important role in P2X7R mediated cellular function and need to be explored further.

In Chapter 3, using Lucifer yellow we confirmed that prolonged stimulation of P2X7R induced pore formation in astrocytes. Pore formation was augmented in the absence of extracellular calcium, a fundamental property of P2X7R. In this chapter, using ethidium bromide (EtBr), a high molecular weight dye, we further probed whether the pore formation activity involves P2X7R or Panx-1. EtBr mainly enters and binds to the DNA of apoptotic cells but in normal cells, the EtBr entry into the cells is predictive of membrane permeabilization/pore formation. We showed that 15 min BzATP treatment induced significant EtBr entry in astrocytes whereas it did not cause any change in cellular morphology as observed in phase contrast images of astrocytes captured in the same field, thus indicating membrane permeabilization. We next used various pharmacological blockers including oxATP, A438079 (P2X7R inhibitor), suramin (P2R inhibitor) and probenecid (Panx-1 hemichannel blocker) before BzATP application and observed that P2X7R inhibition or blockade of Panx-1 both significantly suppressed the BzATP induced EtBr uptake by astrocytes (Fig. 5.6.). We further extended our study and checked whether the pore formation also occurs in cultured astrocytes upon exposure to Tat. 15 minute exposure to Tat allows huge entry of Lucifer Yellow and EtBr into the cells indicating membrane permeabilization (Fig.5.7.). We hypothesized that this might be due to pore formation/hemichannel opening which might involve P2X7R activation or Panx-1 hemichannel opening. Hence, for our next experiment we co-applied Tat and EtBr in cultured cells after treating the cells with similar pharmacological blockers as used for BzATP experiments and evaluated the dye uptake. We found a significant decrease in dye uptake with A438079, oxATP and probenecid which was comparable to non-treated cells indicating that Tat-induced pore formation involves P2X7R activation and Panx-1 hemichannel

opening. Additionally, we observed that the attenuation was even more (below control) when cells were pretreated with suramin suggesting that other purinergic receptors are also involved in the process (Fig. 5.8).

The hemichannel opening in astrocytes is related with ATP release which occurs downstream to P2X7 receptor activation and the reverse phenomenon that ATP released upon hemichannel opening activates P2X7R activation is also acceptable in certain conditions (Jackson, 2015). In our experiments, we showed that Tat-mediated ATP release occurs upon P2X7R activation. As P2X7R form functional complexes with Panx-1, as revealed by coimmunoprecipitation (Fig.5.5.), we further evaluated whether hemichannels are playing any role in Tat-induced ATP release. Treatment of cells with carbenoxolone (CBX) significantly reduced Tat-induced ATP release. However, it did not pose any effect on basal ATP release (Fig.5.9.A). To clearly demonstrate the role of particular hemichannel type involved, we treated cells with Probenecid and Gap 26, which specifically block Panx-1 and Cx43, respectively. We found a minor decrease in ATP release with probenecid but Gap26 significantly reduced the ATP almost near control levels (Fig. 5.9 B). This suggested that Cx43 hemichannels, not the Panx-1 channels mediate Tat-induced ATP release from astrocytes. To further confirm the role of connexin-43 in the process, we knocked down the Cx43 in astrocytes using specific siRNA against Cx43. Western blot data confirmed significant knockdown of Cx43 after 24 hr. Furthermore, ATP release assay revealed that Cx43 siRNA significantly suppressed the Tat-induced ATP release, suggesting that Cx43 hemichannel opening is indeed involved in the ATP release process. Connexin hemichannel-mediated ATP release has also been shown in different tissues including cochlea, cornea and peripheral nervous system (Gomes et al., 2005; Zhao et al., 2005; Nualart-Marti et al., 2013b). Dysregulated hemichannel activity has been linked to neuroinflammation characterized by microglial and astrocyte activation and release of inflammatory cytokines from activated cells (Kielian, 2008; Takeuchi and Suzumura, 2014). This suggests that hemichannel plays a dual role in regulating molecular homeostasis in the context of neurodegenerative diseases. On the one hand, transient hemichannel activity has been suggested to be protective during normal physiologic states as well as acute

insults or inflammation. Conversely, sustained hemichannel opening during chronic neurodegenerative diseases may promote disease progression by perturbing metabolic gradients and the exaggerated release of toxic molecules from activated glial cells and neurons to induce cell death. This can result in the cognitive decline or motor abnormalities in the affected individuals depending which area of the brain is affected. During HIV infection, gap junction channels have been shown to spread toxic signals from infected astrocytes to distant astrocytes, neurons or endothelial cells via gap junction channel (Eugenin and Berman, 2007; Berman et al., 2016). Additionally, it is also demonstrated that connexin-43 hemichannel opening upon HIV-1 infection leads to the release of dickkopf (DKK1) protein from astrocytes that lead to the neuronal damage (Orellana et al., 2014). Our results provide evidence for the role of Cx43 in ATP release in cultured astrocyte during HIV neuropathogenesis, thus, connexin-43 hemichannels could be an important area to be studied with regard to HIV-1 neuropathogenesis which might cause astrocyte dysfunction or else may be a consequence of its overactivation.

Glutamate is another most potent neurotoxic factor released from activated microglia and astrocytes during pathological conditions. Excessive glutamate has been shown to induce neuronal damage via excitotoxicity. It is also one of the major pathways in HIV neuropathogenesis. BzATP/ P2X7R stimulation has been shown to release glutamate from astrocytes. We, therefore, tried to investigate whether inhibiting P2X7R will reduce the Tat-induced increase in glutamate level. In accordance with earlier reports, we also observed a significant increase in glutamate release upon exposure of astrocytes with Tat. All the tested P2X7R inhibitors significantly reduced glutamate levels in the extracellular media suggesting the involvement of P2X7R activation in glutamate release.

Our experimental data provide strong evidence that Tat treatment leads to enhanced ATP and glutamate release from astrocytes resulted due to activation of the P2X7 receptor. We further checked the possibility whether Tat-induced indirect neuronal apoptosis might be due to excessive release of ATP and glutamate in astrocyte conditioned media which binds to and activates neuronal purinergic and glutamatergic

receptors, respectively. Blockade of the neuronal purinergic receptor with suramin or glutamatergic receptor with NMDA receptor blocker APV reduced Tat-treated ACM-induced neuronal death. To further confirm the role of ATP in neuronal death, 30 minutes prior to collection of astrocyte conditioned media, we abolished the ATP in conditioned media by treatment with apyrase, which hydrolyzes ATP into ADP and AMP. We observed that apyrase treatment to astrocytes also significantly reduced Tat-induced indirect neuronal death. Application of apyrase and APV or suramin and APV together did not cause any synergistic reduction in neuronal death as compared to their individual effect. This suggested that ATP and glutamate released from astrocytes are either acting independently to each other or one of them is acting downstream to other and hence posing similar effect. However, this is planned to be critically analyzed further in the lab in future.

These findings have provided new insights into the role of P2X7R activation in enhanced release of ATP and glutamate from astrocytes upon exposure to Tat which subsequently led to neuronal apoptosis. Since neuronal apoptosis due to astrocyte dysfunction is a major mechanism for HIV-induced neurodegeneration, blockers of purinergic receptors can be considered for therapeutic interventions. The elucidation of the role of Cx43 and Panx-1 hemichannels in Tat-mediated effect also highlights the importance of P2X7R-hemichannel association in astrocytes and would need further explorations for improved understanding of HIV neuropathogenesis. These findings have far-reaching implications in HIV/AIDS patients suffering from HAND.